

# Design and Implementation of a Linear Motor for Multi-Car Elevators

Ahmet Onat, *Member, IEEE*, Ender Kazan, Norio Takahashi, *Fellow, IEEE*, Daisuke Miyagi, *Member, IEEE*, Yasuhiro Komatsu and Sandor Markon, *Member, IEEE*,

**Abstract**—The multi-car elevator system is a revolutionary new technology for high-rise buildings, promising outstanding economic benefits, but also requiring new technology for propulsion, safety and control. In this paper we report on experimental results with new components for linear motor driven multi-car elevators. We show that linear synchronous motors with optimized design and with our new safety and control system can be considered as core components of a new generation of elevator systems. The main new results concern the development of a safety system integrated into the propulsion system, the design methodology of a linear motor optimized for the multi-car elevator task, and the motion control system that is expected to be usable for extra high-rise buildings.

**Index Terms**—Linear motors, elevators, safety methods, design optimization

## I. INTRODUCTION

MULTI-CAR elevator systems with independently moving elevator cars in the same hoistway hold the promise of large improvements in the space utilization of urban buildings. Currently, a large amount of potentially useful floor space is consumed by elevator shafts, each of which runs single elevators in huge empty spaces spanning many floors. Multi-car elevators would allow architects to reclaim a large proportion of that space, by moving many of the single elevators into common shafts. This effect is especially pronounced in ultra high-rise buildings, where the elevator space ultimately becomes the limiting factor for economical feasibility. There is already a two-car elevator system on the market, implemented by using conventional traction drive elevator technology. However, for obtaining substantial improvements over single-car systems, multi-car elevators should convert three, four, or more banks of zoned single-car systems into integrated multi-car systems. For this, we should be able to use three or more cars, in hoistways spanning several hundred meters [1]–[4]. To realize such huge scale multi-car systems, a new technology is needed, which can be realized by linear motors [5].

Design of linear motors have been studied for several decades [6], mostly in the context of industrial drives [7]. Vertical transportation applications have also been investigated, especially recently [8]–[11], and one major topic has been

the design of linear motors with a high ratio of payload to self weight. Synchronous motors are more suitable for this application, and in many cases either switched reluctance motors (SRM) or permanent magnet synchronous motors (PMSM) have been used. Although SRM motors have been used for this application [12], [13], an iron core is required and thrust to weight ratio is low. For our application, the best solution appears to be using permanent magnet linear synchronous motors [9], [10], [14]–[16], which are also used in our research.

In this paper, we propose a new linear motor specifically designed for multi-car elevator applications. One of our primary requirements is providing a reliable safety system, while keeping the total cost economically feasible. This is achieved by the dual use of the linear motor stator, both as a propulsion component, and as the actuator device for the mechanical safety system. This idea, first reported at [17], [18], has been analyzed and experimentally verified, as described in Section II. The second requirement is optimizing the design with respect to material and energy costs and reducing noise and vibration, while keeping it easy to manufacture. This is achieved by a multi-objective optimization procedure described in Section III. The theoretically predicted performance is verified by measurements on an actually implemented full-scale model, as given in Section IV. We have also developed a simple but effective control system, which is described in Section V, and the test results given in Section VI, on the experimental results for its performance.

## II. SAFETY SYSTEM FOR LINEAR MOTOR ELEVATORS

For the safety of boarding and leaving passengers, elevators must be positively held during stops at service floors. Usually, elevators have electromechanical brakes installed at a stationary position to hold safely the traction motor, independently of power and control issues. An equivalent stationary brake device for linear motor elevators, capable of mechanically stopping and holding the elevators at any floor, would need to span the whole hoistway, and would be too expensive. On the other hand, if a mechanical brake is installed on the elevator car, the signal and power for its actuator would need to be transmitted to the moving car using cables moving with the car, which might raise reliability concerns and is undesirable in a multi-car elevator system since they would interfere with the operation of the other cars.

Our solution is to put the mechanical parts of the brake on the car, but keep the actuator on the hoistway side, thus

Ahmet Onat and Ender Kazan are with the Faculty of Engineering and Natural Sciences, Sabanci University Istanbul, 34956 Turkey

Norio Takahashi and Daisuke Miyagi are with the Department of Electrical and Electronic Engineering, Okayama University, Okayama 700-8530, Japan  
Yasuhiro Komatsu is with the Department of Electrical Engineering, Ritsumeikan University, Shiga 525-8577, Japan

Sandor Markon is with the Graduate School of Information Technology, Kobe Institute of Computing, Kobe 650-0001 Japan

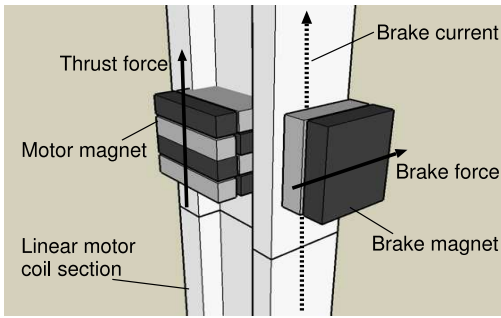


Figure 1. The safety system using stator top edge as a brake actuator.

avoiding the signal and power transmission problem. This arrangement would still be expensive if we used a separate, long, actuator device along the hoistway. However, we already have a long device spanning the hoistway: The stator of the linear motor, assuming that we use a long armature type motor with permanent magnet movers. The long armature is available to serve as the actuator for the brakes, and incidentally, it can also be put to service for many other uses, e.g. for power and signal transfer to the elevator cars.

In our research, we have developed a safety system for multi-car elevators, with the unique feature of using the top edge of the stator as the actuator solenoid of the brakes. In the following, we report on theoretical analysis and test results, showing the feasibility of this approach.

#### A. Actuator and Brake Operation

Special DC bias currents superposed on the drive currents can be used to generate a brake current along the top edge of the stator which cause a force on a permanent magnet in its vicinity (Fig. 1). The permanent magnet is in turn connected to a brake mechanism. Details of the bias currents will be explained in Sec. II-B.

When the mover is to be manipulated, DC bias currents to release the brake are supplied together with the normal drive currents. To hold the mover at a given position for a long time, the bias currents may be removed to engage the mechanical brake. The primary function of this brake will be to hold stopped elevator cars under normal operating conditions. In an abnormal situation such as a malfunction including loss of power, since the bias currents cannot be applied properly, the mechanical brake will engage, arresting the fall of the mover.

Using this method it becomes possible to generate thrust and operate the brake mechanism on the same part of the motor section. Another obvious solution is to use separate motor sections for generating thrust and for operating the brake. However, this method is not preferred in this paper since the required mover length would be long.

In a multi-car elevator system, it is necessary to ensure that two cars are not accidentally driven into each other. This brake can also be used to construct such a safety system, by using the mechanical brakes on each elevator and controlling the actuator force of each section of motor. Assuming that there are  $n$  stator segments, at most  $n$  zones along the motor

can be set up where the brake actuator force is controlled independently. By suitable interlocks using the bias currents supplied to adjacent zones, there will always remain a “locked” zone between any two elevator cars. Since the mechanical brake will stop a car if it is not released by the actuator force, no car can approach another, closer than one zone distance. This property guarantees that collisions cannot occur.

#### B. Magnetic Field of the Linear Motor Coil

We consider a coreless 3 phase linear motor stator assembly made up of coils as shown in Fig. 2. We can approximate the coils as coplanar rectangular current paths.

For the case of a coil of the stator with its winding along the path  $L$  on the top edge of the stator winding, the magnetic field generated by the current  $I_L$  at a point  $\mathbf{r}$  in the absence of magnetic material can be calculated directly from Biot-Savart’s law:

$$\mathbf{B}(\mathbf{r}) = \frac{\mu_0 I_L}{4\pi} \int_L \frac{d\mathbf{L} \times (\mathbf{r} - \mathbf{x})}{|\mathbf{r} - \mathbf{x}|^3} \quad (1)$$

In [19] we find an explicit formula integrating (1) for coplanar rectangular coils, which is a good approximation of the coreless linear motor stator. Using these formulas, we obtain the magnetic field distribution in the vicinity of the stator top.

For the case of identical DC currents injected into each coil, the field distribution along the stator top is similar to the field around a single long straight conductor spanning the length of the motor. Therefore, if a permanent magnet is placed in this region with one pole facing the stator top surface, there will be predominantly a sideways force acting between the coil and the magnet, which can be used for brake operation.

When the coils are fed balanced 3 phase currents, the force on a magnet spanning at least one pole pair will balance out, with the net braking force near zero. However, when we superpose a DC bias current on each phase, their contribution will add up to a net brake force. Thus, this superposed DC current is available as an independent control variable that directly operates the brake. The brake force will be approximately constant along the length of the stator, as seen from the experimental data in Fig. 16 in Sec. VI, and dependent only on the DC bias currents.

#### C. The Effect of Winding Pattern

A problem may be encountered in implementing the brake actuator in practice because the field distribution at the top edge of a linear motor stator depends on the actual winding pattern of the coils. The above analysis applies to the case of identical coils arranged at  $120^\circ$  electrical degrees, which we will call here “balanced winding”. This winding pattern is shown schematically in Fig. 2 where  $i_a, i_b, i_c$  are the three phase currents. Note that the actual coil shapes are different, e.g. the coil sides lay in the same plane, and the top edges of the coils have complex 3 dimensional shapes (see Sec. IV.)

However, a preferred winding method used in the industry which we call “segmented winding” (implementing a different scheme where two phases are wound at  $120^\circ$  degrees, but

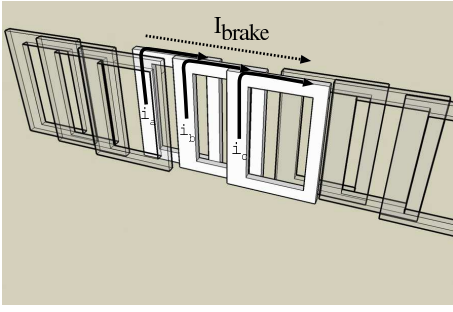


Figure 2. Balanced winding pattern of linear motor coils.

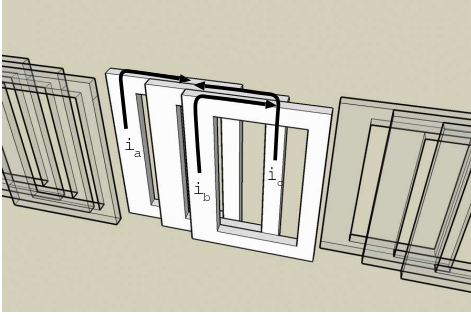


Figure 3. Segmented winding pattern of linear motor coils.

the third phase placed at the  $60^\circ$  position, and fed a reversed current as shown in Fig. 3) is advantageous because it is easier to separate the winding into sections, thus being simpler to manufacture.

For balanced winding type stators during normal running with balanced currents, the average current generating the stator top field is zero. If the neutral point of the motor winding is tapped to sink a DC current component through all coils, which we call the brake current  $I_{brake}$ , supplied through the motor terminals, the average current vector now becomes nonzero for *any* value of  $I_{brake}$ .

$$I_{brake} = i_a(t) + I_{DC} + i_b(t) + I_{DC} + i_c(t) + I_{DC} \quad (2)$$

where  $i_a(t) + i_b(t) + i_c(t) = 0$  are normal balanced drive currents. Therefore,  $I_{brake} = 3I_{DC}$ .

Using this method, the brake currents on the balanced winding can be created independently of drive currents.

For segmented winding on the other hand, the total stator top field is non-zero during normal running when driven with balanced currents  $i_a(t) + i_b(t) + i_c(t) = 0$ , since the top field of the  $60^\circ$  coil will be opposite to the other two phases. It is possible to cancel the stator top field by supplying a special non-balanced current vector satisfying  $i'_a(t) + i'_b(t) - i'_c(t) = I_{DC}$ , where  $i'_c$  is the current in the  $60^\circ$  coil, and  $I_{DC}$  is a constant current. The non-balanced currents also require that the neutral point of the motor be tapped.

The balanced winding is better suited for a safety brake operation on linear motor elevators since generating a stator top field requires a special current pattern. The segmented winding on the other hand, will generate a zero stator top field in one special case current. In case of emergency where

the motor or the motor driver is damaged or power is lost, there is a larger set of possible failure modes in which the balanced winding will not be able to provide the special current pattern and thus the brake will engage to arrest the fall of the elevator car. Calculated DC currents necessary for different brake operations are given in Table I.

Another advantage of balanced winding is that since the system is set up in such a way that brake is engaged for zero brake current and disengaged when brake current exceeds a certain value, there is no need to supply brake current when the elevator car must be stopped.

Table I  
DC CURRENTS FOR DIFFERENT OPERATIONS

Elevator	Driven (lifting)	Brake Active	Segmented Winding	Balanced Winding
Moves	Yes	No	$(4i'_a - I_{DC})/3$	$I_{brake}$
Stops	Yes	No	$(4i'_a - I_{DC})/3$	$I_{brake}$
		Yes	$4i'_a/3$	0
	No	Yes	0	0

### III. MULTI-OBJECTIVE OPTIMIZATION OF THE DESIGN OF AN ELEVATOR LINEAR MOTOR

The major part of the cost of a linear motor elevator drive is the stator, since it has to span the whole hoistway length. To minimize the active material required for constructing the stator, the natural choice is to use an air-core permanent magnet synchronous motor. There are two important subjects of decision in the design of a multi-car linear motor elevator which have effect on the installation cost of the end-product. The first is whether the stator is made up of windings or magnets. Here, we have selected the former since it is not practical to attach cables to the movers, as previously discussed. The second cost factor after this decision is to design the mover to minimize the cost of the movers, which is dominated by the weight of the magnet. In this section, we investigate the optimal design of such a motor for multi-car linear motor elevator applications [15].

Two kinds of movers for the air-core linear PM synchronous motors are investigated; one with Halbach type permanent magnet arrangement and the other, iron yoke and permanent magnets, shown in Figs. 4(a) and (b).

The reduction of the ripple of driving force is required in the practical utilization of linear synchronous motor for rope-less elevator. In addition, it is important to increase the driving force and to reduce the weight of motor. Then, the optimal design of linear motor is examined including multi objective criteria, in order to meet these design requirements. We note that a related research has been reported in [20], but this is without using multi objective optimization and considering only yoke-type design. Other methods also exist in the design of permanent magnet actuators [21], [22].

#### A. Halbach-Type Linear PM Motor (HTLPM)

The dimensions of the analyzed model of HTLPM are shown in Fig. 4(a). The gap length between the magnet and the coil is 4 mm. One period of 3 phase alternating current

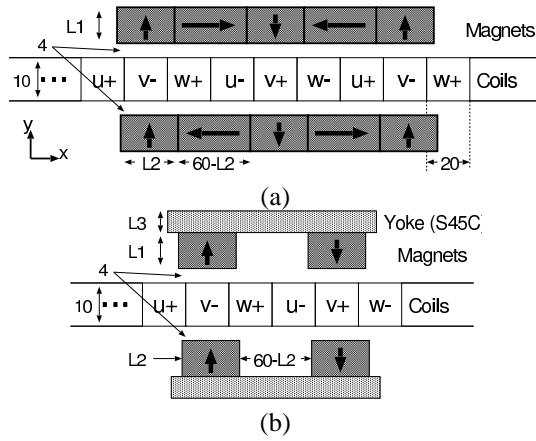


Figure 4. Examined linear motor. (a) Halbach type. (b) Yoke type. (units in mm)

is equal to a movement distance of 120 mm. The amplitude of current density  $J_0$  in the 3 phase system is  $3.0 \times 10^6$  A/m<sup>2</sup>. The calculation by Biot–Savart’s method is performed at every 5 mm displacement of the magnet region in the 3-dimensional magneto-static field, resulting in a total of 24 calculation steps. The value of  $x$  component of the force in each step is calculated by the BIL law.

The design variables are chosen as the dimensions of the magnets ( $L_1$ ,  $L_2$ ) as shown in Fig. 4(a). The dimensions of the magnets were limited as  $0 \leq L_1 \leq 50$  and  $0 \leq L_2 \leq 60$  in mm. The optimization is carried out using the evolution strategy (ES) method [23]. In (1+1)–ES, we generate one child vector from one parent vector, comparing the objective functions of each vector. The vector with a dominant objective function is treated as a parent vector of the next generation.

Three functions,  $W_1$ ,  $W_2$  and  $W_3$ , are used for the optimization according to the criteria stated above:

$$W_1 = 1/F_{xave} \quad (3)$$

$$W_2 = W_g \quad (4)$$

$$W_3 = r_d = (F_{xmax} - F_{xmin})/F_{xave} \times 100 \quad (5)$$

where  $F_{xmax}$ ,  $F_{xmin}$  and  $F_{xave}$  are the maximum, minimum and average values of  $x$  components of force at each step,  $W_g$  is the weight of magnet and  $r_d$  is the force ripple. The objective function,  $W$ , is the linear combination of  $W_1$ ,  $W_2$  and  $W_3$  as follows:

$$W = k_1 W_1 + k_2 W_2 + k_3 W_3 \quad (6)$$

In order to get a similar contribution from each function, the weighting coefficients  $k_1 \dots k_3$  are determined so that the following relation is satisfied:

$$k_1 W_1 = k_2 W_2 = k_3 W_3 \quad (7)$$

Table II shows the result of optimization. The force ripple is improved from an initial value of 4.83% to 0.2%, whereas the weight of the magnet is increased from the initial value. If  $k_1$  in (6) is increased and the optimization is carried out,

Table II  
DIMENSIONS, THRUST, ETC.

	Initial shape	Optimal shape
$L_1$ (mm)	10	30
$L_2$ (mm)	30	20.9
$F_{xave}$ (kgf)	40	71.9
$W_g$ (kg)	6.3	18.1
$r_d$ (%)	4.83	0.2
$\eta$	0.343	1.867

Table III  
THRUST, WEIGHT, ETC. (HALBACH-TYPE,  $L_2 = 20$  MM)

L1	F(kgf)	Q	W	P	$\eta_1$	N	Ci	Cr
10	36.34	6	6	30.34	5.06	6.6	39.56	6.6
20	58.4	12	12	46.4	3.87	4.3	51.73	4.3
30	71.63	18	18	53.63	2.98	3.7	67.12	3.7

the optimal result having larger force  $F_{xave}$  will be obtained, and vice versa.

In this optimization, there are three objective functions,  $W_1$ ,  $W_2$  and  $W_3$  as shown in (3)–(5). This is the multi-objective optimization (MO) problem. Unlike the single objective optimization, the solution of MO problem is not a single point, but a family of non-dominated points known as the Pareto optimal solutions [20]. In general, there is a trade off relationship among the objective functions and it is difficult to minimize the objective functions  $W_1$ ,  $W_2$  and  $W_3$  simultaneously. Accordingly, MO problem is to find as many different Pareto optimal solutions as possible.

Figure 5 shows the Pareto optimal solution for the multi objective optimization problem of  $W_1$  ( $1/F_{xave}$ ) and  $W_2$  ( $W_g$ ). In this case, the ripple  $r_d$  of driving force is not optimized. We describe the concept of Pareto optimal solutions using Fig. 5, where both objectives  $W_1$  and  $W_2$  are minimized. Each point on the boundary in the feasible region is the optimal solution in the sense that no improvement can be achieved in one objective that does not lead to degradation in at least one of the remaining components. From the viewpoint of small  $W_1$  (large thrust) and small  $W_2$  (light mover), the result near point A in Fig. 5 is a Pareto optimal solution. The force magnification factor  $\eta_1$  of the linear motor is given by (8), where  $\eta_1 > 0$  means that the linear motor can lift the required weight.

$$\eta_1 = (F_{xave} - (W_g + 20)) / W_g \quad (8)$$

The factor for a desired payload of 20 kg/mover is shown in Fig. 6 for the Pareto optimal solution. In this case, the force magnification factor  $\eta_1$  becomes the maximum at about  $W_g = 10$  kg. The thrust, weight, etc. of some of the Halbach type movers are shown in Table III.

The main cost of the linear motor mover is the NdFeB magnet which is proportional to  $W_g$ . From Figs. 5 and 6, a designer can determine the parameters of a linear motor considering the cost and the required thrust.

### B. Yoke-Type Air-Core Linear PM Motor (YTLPM)

In the air-core linear PM motor with the mover yoke made of carbon steel (S45C) shown in Fig. 4(b), the thickness  $L_3$

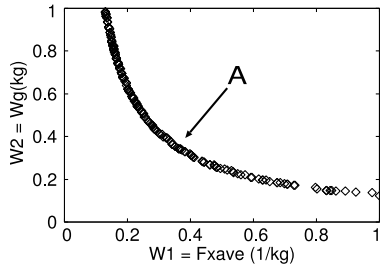


Figure 5. Pareto optimal solution.

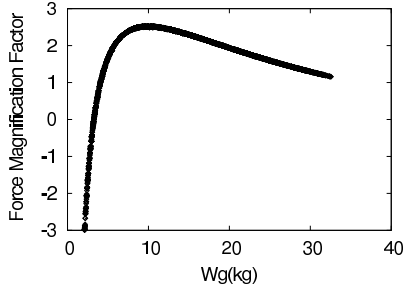


Figure 6. Force magnification factor of Halbach type motor.

of the yoke is treated as a design variable. Of the remaining two parameters, the width of the magnets  $L_2$  is fixed at 20 mm which is close to the optimal value, and the thickness of the magnets  $L_1$  is also left free as a design variable. The flux distribution and the thrust are calculated by using the 3D finite element method taking into account the nonlinear B-H curve of the yoke.

Let us assume that the required payload is 200 kg including the weight of the cage and passengers. The payload per mover  $P = F - Q$ , the force magnification factor  $\eta_2 = P/W_g$ , and the required number of units of linear motor movers  $N = 200/P$  are the motor parameters where  $F$  is the thrust per mover,  $Q$  is the total weight of one mover, and  $W_g$  is the magnet weight. For the optimal design, the performance of the motor is calculated for various combinations of  $L_1$  and  $L_3$ , as shown in Table IV. The initial cost and the running cost are proportional to  $C_i = 200/\eta_2$  and  $C_r = N$ .

Table V shows the thrust  $F$ , total weight  $Q$ , etc. at  $L_2 = 20$  mm for the models shown in Table IV. The results of Tables V and III are plotted in Fig. 7. The running cost  $C_r$  can be reduced by using the Halbach type mover (HTLPM), and the initial cost  $C_i$  can be reduced by using the yoke type mover (YTLPM). If the initial cost  $C_i$  has the highest priority, then model 1 is the most appropriate in Table V, as signified by  $\eta_2$ . For obtaining large thrust and small running cost, the Halbach type mover is better, although the yoke type provides a small initial cost where stator cost is the same for each.

Table IV  
EXAMINED COMBINATION OF  $L_1$  AND  $L_3$  ( $L_2 = 20$  MM)

Model	1	2	3	4	5	6	7	8	9
$L_1$	10	10	10	20	20	20	30	30	30
$L_3$	5	10	15	5	10	15	5	10	15

Table V  
THRUST, WEIGHT, ETC. (YOKE-TYPE,  $L_2 = 20$  MM)

Model	F(kgf)	Q	W	P	$\eta_2$	N	$C_i$	$C_r$
1	26.38	5.4	2.4	20.98	8.74	9.5	22.88	9.5
2	29	8.4	2.4	20.6	8.58	9.7	23.3	9.7
3	29.33	11.4	2.4	17.93	7.47	11.2	26.78	11.2
4	32.66	7.8	4.8	24.86	5.18	8	38.61	8
5	35.58	10.8	4.8	24.78	5.16	8.1	38.74	8.1
6	36.24	13.8	4.8	22.44	4.68	8.9	42.77	8.9
7	35.7	10.2	7.2	25.5	3.54	7.8	56.46	7.8
8	37.87	13.2	7.2	24.67	3.43	8.1	58.38	8.1
9	38.55	16.2	7.2	22.35	3.1	8.9	64.43	8.9

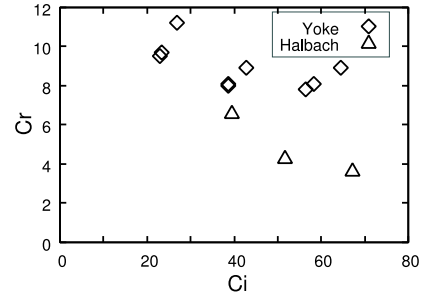


Figure 7. Comparison of initial cost  $C_i$  and running cost  $C_r$  ( $L_2 = 20$  mm).

As a result, the composition shown in Fig. 8 was adopted. The yoke between magnet pairs is omitted in order to reduce the weight. The flux distribution obtained by using the finite element method shown in Fig. 9 displays some leakage flux because the yoke is saturated (maximum flux density: about 2T). This design provides 33.8 kgf of thrust  $F$  for 4.8 kg of mover weight  $Q$ , of which 2.93 kg is the magnet weight, and  $L_1 = 10$  mm and  $L_3 = 10$  mm.

#### IV. IMPLEMENTATION OF THE LINEAR MOTOR

In this section, the design and implementation of the motor coil shape and a special motor driver that can produce the necessary currents to generate the brake force for the full scale motor that was used in the experiments will be given.

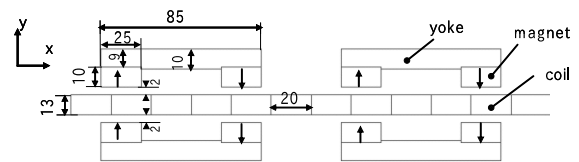


Figure 8. Adopted composition. (units in mm)

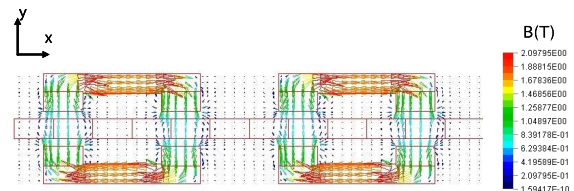


Figure 9. Flux distribution.



Figure 10. Balanced winding pattern implemented as final design.

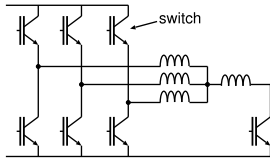


Figure 11. Suggested motor driver for brake operation.

Several possibilities exist in implementing the coil shape for the motor with the requirements discussed. After considering three preliminary coil shape designs, we have arrived at the final design shown in Fig. 10 which is of the balanced type. The design intends to simplify construction by utilizing only one coil shape that is repeated.

Considering the motor driver for the balanced winding pattern, it becomes clear that it is not possible to supply  $I_{DC}$  currents to each coil using conventional 3 phase motor drives with standard bridges and vector control, since the motor neutral point is isolated. One solution is using an additional switch for the common point to ground or DC link as shown in Fig. 11. To start producing the brake currents, first the time during the PWM cycle when all the top switches are closed (which we will call  $T_3$ ) is reduced to zero, then the motor neutral point is connected to ground through a ballast inductor, and finally time  $T_3$  is reset to a value for a suitable brake current. Using this method, the generated current patterns can be seen in Fig. 12, which are the regular drive waveforms but with an offset.

## V. MOTOR CONTROL

### A. Position Control method

Our control system for linear motor elevators has been designed by making use of some specific properties of the problem.

First, we note that in contrast with the traditional elevator system, where the unbalance load of the elevator car and

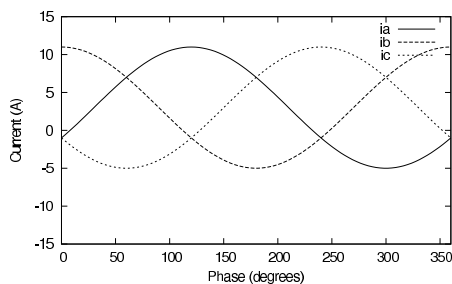


Figure 12. Current waveforms for brake operation.

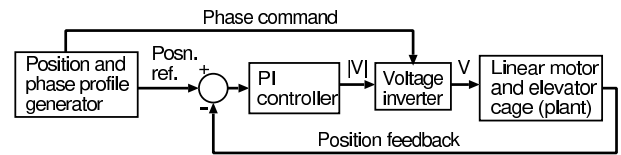


Figure 13. Block diagram of the position control system.

the counterweight could point either upwards or downwards, here we always deal with downwards loads. The system thus operates only in two quadrants, “motoring upwards” or “generating downwards”. Furthermore, the weight of the elevator car together with the mover provides a substantial base load, even with an empty car. This allows us to use a very simple minded position control loop, without the need to worry about switching between quadrants, as during one trip the system always operates in a single quadrant.

To render the system robust in the event of degraded quality for the position signal, which might occur with some of the position sensing methods that can be used, we dictate the phase of the armature current, just like in the case of open loop control, and control only the current amplitude. In case the position signal deteriorates, the current amplitude command can latch up to the allowed maximum, and the elevator can continue its trip under open loop operation. The schematic block diagram of the experimental system is shown in Fig. 13.

Note that the usual nested current and speed control loops have been eliminated and instead, only the position is controlled through the inverter voltage command. This simple setup was chosen to allow implementation on low cost microprocessors with relatively low computing capacity. This is needed since a distributed control system is to be implemented as discussed below, which must be economically feasible.

Our test results show that this control system can still achieve sufficient performance levels in spite of its simplicity.

### B. Distributed Control of the Motor

The linear motor is designed to be driven in a modular way such that an arbitrary length of motor can be produced and multiple elevator cars manipulated independently. The simplest method for driving such a motor is to implement a centralized control scheme where each module is directly connected to a central controller. However this approach can only be applied to a limited number of movers in the system. Therefore, control of the movers should be shared across local controllers instead of one master controller.

If a mover is going to traverse a certain part of the motor, relevant segments along the way must be allocated and freed as necessary with a predetermined timing to avoid collisions as well as allowing for high utilization of segments. For this work, a central coordination mechanism was selected for simplicity, but it will be replaced by a distributed mechanism later for scalability, using a real-time computer network to synchronize electrical phase timing.

In the present implementation, to move an elevator car in a multi-car elevator system from one floor to another, first segments of the motor between these locations are checked to

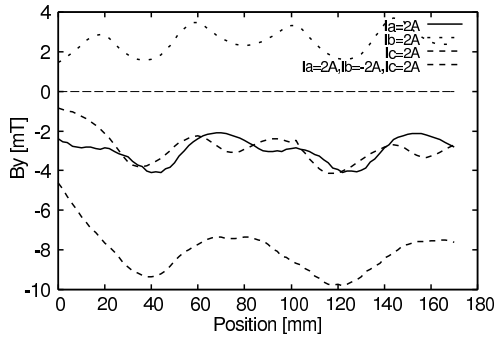


Figure 14. Experimental stator top field distribution of Motor 1.

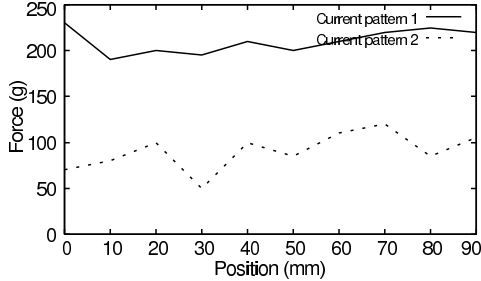


Figure 15. Experimental brake force distribution of Motor 1.

be available by a central coordinator, then they are reserved for this motion, and finally the cage is moved by the coordinated interaction of all of the controllers in the reserved region.

## VI. RESULTS

In this section results pertaining to two different motors will be given: The small scale linear motor model purchased for initial tests “Motor 1”, having the segmented winding pattern, and the full scale motor designed under the guidelines set forth in this paper, having the balanced winding pattern “Motor 2”.

The stator top field produced by Motor 1 with respect to position in the direction of motion can be seen in Fig. 14 for each coil excited separately with a constant current. The field produced with all phases excited with constant current is also shown as the lowest plot in the figure. It can be seen that the latter has large variation.

The force generated by the stator top field obtained by supplying the modified current  $i_a + i_b - i_c = I_{DC}$  was also measured with respect to the motor position. It can be seen in Fig. 15 that we can supply precise currents to keep the stator top magnetic field relatively constant.

After Motor 2 was designed and constructed, tests were carried out for the magnitude and uniformity of the brake force and payload capacity. The uniformity of the force generated at the top of the stator for the brake operation of Motor 2 was measured. A magnet plate with the length of one electrical phase and with the width equal to the stator width was built using N38 type magnets. It was attached to the mover via a linear bearing enabling motion perpendicular to the plane of the stator, and connected in such a way that the generated force was applied to a strain gage. The terminals of the motor were reconnected so that the same magnitude DC current could be

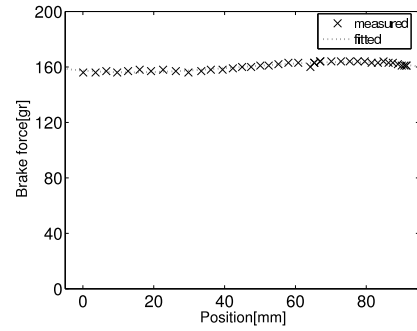


Figure 16. Experimental brake force distribution of Motor 2.

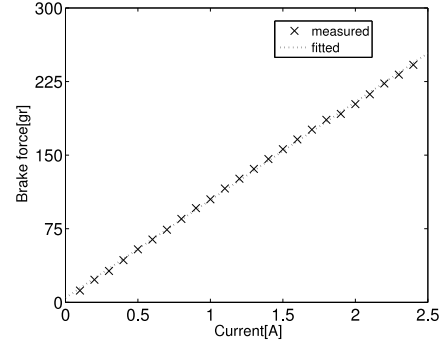


Figure 17. Generated brake force with respect to brake current, Motor 2

applied to each winding separately, creating the desired stator top magnetic field. The resulting sideways force on the magnet plate was measured. The results can be seen in Fig. 16. As the mover changes position, the generated force is nearly constant, and therefore suitable for the brake operation. It can also be seen that the force is not large. Therefore, a brake mechanism with finely adjusted mechanical advantage must be used. The force can be increased through a larger magnet plate or a better magnetic design.

Finally, the change in the brake force with respect to  $I_{brake}$  while the mover is stopped at one location is shown in Fig. 17. Since the force changes almost linearly, it can be said that the brake actuation is independent of the normal drive currents, and can be controlled by the DC current component applied to the motor using a suitable motor driver, such as the one described in section IV. The experimental results for both Motor 1 and Motor 2 agree with the analysis given previously.

Lastly, the payload capacity of Motor 2 was tested by applying a fixed motor current of 3 A (max) to the stator and measuring the position of the mover with respect to the motor phase while increasing the load force. Since the motor is oriented vertically, as the load was increased, the mover shifted to a lower position. The results can be seen in Fig. 18. The mover made up of N38 type magnets (labeled “N38 single”) is capable of lifting a maximum of 8 kg. The only difference between the mover labeled “N38 single” and “N45 single” is the type of magnets. The latter, made up of stronger N45 magnets can lift up to 11 kg of payload. The dependence of the motor load capacity with respect to magnet type can be clearly seen. It can be inferred from this result that the operating costs of the system, mainly the electrical power requirement can be

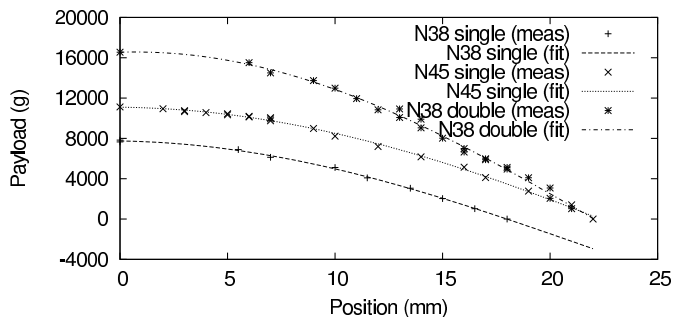


Figure 18. Measured force vs. displacement (3 A), Motor 2.

reduced by using a mover with stronger magnets. In the future, Halbach array type of magnetic design will be substituted to further increase the payload capacity.

The payload capacity can also be increased by mechanically coupling several movers together, each separated by the distance of one electrical phase, to add up their thrusts. This can be seen in Fig. 18, curve labeled “N38 double”, where two coupled movers made up of N38 type magnets are measured to lift up to 16.5 kg, which is as expected, approximately double the capacity of a single N38 type mover. Enough movers can be connected in this manner to obtain the required thrust, taking care to ensure the correct spacing between movers. Using ten mover units, a payload of 97 kg was obtained, enough to support the weight of one person.

Mechanically coupling mover units may be an inexpensive way of improving payload capacity compared to using a Halbach array [24] since construction is simpler. However, the volume of magnets used in Halbach design is smaller for a given payload capacity.

## VII. CONCLUSIONS

In this paper a new permanent magnet synchronous linear motor concept for linear motor elevators was introduced. A linear motor design capable of generating a magnetic field decoupled from the thrust generating magnetic field of the linear motor was given. The decoupled field can be used to actuate a brake mechanism, forming the basis of an elevator safety system. The idea was supported by a methodology of designing the motor for a desired objective, providing winding patterns and drive methods, followed by simulations and experiments on an actual linear motor designed from the results.

It has been observed that the proposed system can successfully operate as a combined propulsion and safety system. Further research will be done to validate the operation of the safety system for all failure modes, and thus to satisfy the requirements for certification. Furthermore, we are working on the modification of the optimization procedure to include directly the cost of the stator, which will become an important factor when applying the results of this research to extreme high-rise elevators.

## ACKNOWLEDGMENTS

This research was supported in part by Fujitec Co., Ltd. of Japan.

## REFERENCES

- [1] T. Ishii, “Elevators for skyscrapers,” *Spectrum, IEEE*, vol. 31, no. 9, pp. 42–46, 1994.
- [2] W. Jones, “How to build a mile-high skyscraper,” *Spectrum, IEEE*, vol. 44, no. 6, pp. 52–53, 2007.
- [3] S. Markon, H. Kita, and H. Kise, *Control of Traffic Systems in Buildings: Applications of Modern Supervisory and Optimal Control (Advances in Industrial Control)*. NJ, USA: Springer-Verlag New York, Inc., 2006.
- [4] S. Takahashi, H. Kita, H. Suzuki, T. Sudo, and S. Markon, “Simulation-based optimization of a controller for multi-car elevators using a genetic algorithm for noisy fitness function,” in *The 2003 Congress on Evolutionary Computation, CEC '03*, vol. 3, 2003, pp. 1582–1587.
- [5] M. Miyatake, T. Koseki, and S. Sone, “Design and traffic control of multiple cars for an elevator system driven by linear synchronous motors,” in *Proc. Symposium on Linear Drives for Industry Applications*, no. AP-22, 1998, pp. 94–97.
- [6] I. Boldea and S. Nasar, *Linear motion electromagnetic devices*. Taylor & Francis, 2001.
- [7] L. Lu, Z. Chen, B. Yao, and Q. Wang, “Desired compensation adaptive robust control of a linear-motor-driven precision industrial gantry with improved cogging force compensation,” *IEEE/ASME Trans. Mechatronics*, vol. 13, no. 6, pp. 617–624, 2008.
- [8] J. F. Gieras and Z. J. Piech, *Linear synchronous motors: transportation and automation systems*. CRC Press, 2000.
- [9] H. Yamaguchi, H. Osawa, T. Watanabe, and H. Yamada, “Power supply of long stator linear motors application to multi mobile system,” in *Proc. AMC96*, 1996, pp. 441–446.
- [10] S. Chevailler, M. Jufer, and Y. Perriard, “Linear motors for multi mobile systems,” in *IAS2005*, 2005, pp. 2099–2106.
- [11] A. Cassat, B. Kawkabani, Y. Perriard, and J.-J. Simond, “Power supply of long stator linear motors - application to multi mobile system,” in *Industry Applications Society Annual Meeting, 2008. IAS '08. IEEE*, 2008, pp. 1–7.
- [12] H. S. Lim, R. Krishnan, and N. Lobo, “Design and control of a linear propulsion system for an elevator using linear switched reluctance motor drives,” *IEEE Trans. Ind. Electron.*, vol. 55, no. 2, pp. 534–542, 2008.
- [13] H. S. Lim and R. Krishnan, “Ropeless elevator with linear switched reluctance motor drive actuation systems,” *IEEE Trans. Ind. Electron.*, vol. 54, no. 4, pp. 2209–2218, 2007.
- [14] K. Yoshida and X. Zhang, “Sensorless guidance control with constant airgap in ropeless linear elevator,” in *The 4th International Power Electronics and Motion Control Conference*, vol. 2, 2004, pp. 772–776.
- [15] N. Takahashi, T. Yamada, D. Miyagi, and S. Markon, “Basic study of optimal design of linear motor for rope-less elevator,” in *7th International Conference on Computation in Electromagnetics*, 2008, pp. 202–203.
- [16] K. B. Quan, H. X. Zhen, W. Hong-xing, and L. Li-yi, “Thrust and thermal characteristics of electromagnetic launcher based on permanent magnet linear synchronous motors,” *Magnetics, IEEE Transactions on*, vol. 45, no. 1, pp. 358–362, 2009.
- [17] S. Markon, Y. Komatsu, A. Yamanaka, A. Onat, and E. Kazan, “Linear motor coils as brake actuators for multi-car elevators,” in *International Conference on Electrical Machines and Systems*, 2007, pp. 1492–1495.
- [18] S. Markon, Y. Komatsu, A. Onat, A. Yamanaka, and E. Kazan, “Linear motor coils as brake actuators for multi-car elevators,” in *Proc. LDIA*, 2007, pp. 73–74.
- [19] M. Misakian, “Equations for the magnetic field produced by one or more rectangular loops of wire in the same plane,” *J. Res. Natl. Inst. Stand. Tech.*, vol. 105, no. 4, pp. 557–564, 2000.
- [20] S. Vaez-Zadeh and A. Isfahani, “Multiobjective design optimization of air-core linear permanent-magnet synchronous motors for improved thrust and low magnet consumption,” *Magnetics, IEEE Transactions on*, vol. 42, pp. 446–452, 2006.
- [21] H. Son and K. Lee, “Distributed multipole models for design and control of pm actuators and sensors,” *IEEE/ASME Trans. Mechatronics*, vol. 13, no. 2, pp. 228–238, 2008.
- [22] L. Yan, I. Chen, C. K. Lim, G. Yang, W. Lin, and K. Lee, “Design and analysis of a permanent magnet spherical actuator,” *IEEE/ASME Trans. Mechatronics*, vol. 13, no. 2, pp. 239–248, 2008.
- [23] H. P. Schwefel, *Evolution and Optimum Seeking*. John Wiley & Sons, 1995.
- [24] T. Yamada, N. Takahashi, D. Miyagi, S. Markon, and A. Onat, “Investigation of thrust of rope-less elevator using iron yoke and magnet (in Japanese),” in *Chugoku Branch Convention Record of Related Societies of Electronic and Information Engineering, Japan*, 2008.